LETTER

doi:10.1038/nature09898

Circuit cavity electromechanics in the strong-coupling regime

J. D. Teufel[1], Dale Li[1], M. S. Allman[1], K. Cicak[1], A. J. Sirois[1], J. D. Whittaker[1] & R. W. Simmonds[1]

Demonstrating and exploiting the quantum nature of macroscopic mechanical objects would help us to investigate directly the limitations of quantum-based measurements and quantum information protocols, as well as to test long-standing questions about macroscopic quantum coherence[1–3]. Central to this effort is the necessity of long-lived mechanical states. Previous efforts have witnessed quantum behaviour[4], but for a low-quality-factor mechanical system. The field of cavity optomechanics and electromechanics[5,6], in which a high-quality-factor mechanical oscillator is parametrically coupled to an electromagnetic cavity resonance, provides a practical architecture for cooling, manipulation and detection of motion at the quantum level[1]. One requirement is strong coupling[7–9], in which the interaction between the two systems is faster than the dissipation of energy from either system. Here, by incorporating a free-standing, flexible aluminium membrane into a lumped-element superconducting resonant cavity, we have increased the single-photon coupling strength between these two systems by more than two orders of magnitude, compared to previously obtained coupling strengths. A parametric drive tone at the difference frequency between the mechanical oscillator and the cavity resonance dramatically increases the overall coupling strength, allowing us to completely enter the quantum-enabled, strong-coupling regime. This is evidenced by a maximum normal-mode splitting of nearly six bare cavity linewidths. Spectroscopic measurements of these 'dressed states' are in excellent quantitative agreement with recent theoretical predictions[10,11]. The basic circuit architecture presented here provides a feasible path to ground-state cooling and subsequent coherent control and measurement of long-lived quantum states of mechanical motion.

Despite the prevalence of mechanical oscillators in many practical technological applications, demonstrating and using robust quantum behaviour in these systems has proven exceedingly difficult. Recent experimental and theoretical progress has shown that mechanical states may outlive those produced in other media, making them useful for quantum information processing or for macroscopic tests of the quantum–classical divide. Remarkably, a 6 GHz piezoelectric dilatation resonator with strong capacitive coupling to a superconducting phase qubit, cooled by a dilution refrigerator, has allowed control and measurement of a single microwave phonon[4]. This important result confirms the ability to manipulate mechanical quantum states, but the phonon states were short-lived, surviving for only ~6 ns. For mechanical systems to be practically useful, they must survive much longer than a controlled operation time, which in this case is also about ~6 ns. It is a known difficulty that mechanical resonator performance degrades considerably as the fundamental mode frequency increases[12] and that piezoelectric materials can suffer from high internal losses[4].

These difficulties can be alleviated by using low-frequency (<100 MHz), free-standing flexural oscillators, but they must also be cooled further, below 5 mK, in order to avoid thermal decoherence. This requires active cooling. An analogous situation is encountered for charged ions and their motion in a trapping potential; here, a sideband cooling technique brings the system to its motional ground state[13]. The interaction between different ions through their long-lived collective motion is crucial to facilitate quantum information processing. Optomechanics strives to achieve this type of performance, but with ion motion replaced by a macroscopically large mechanical oscillator, and the internal states of ions replaced by a high-frequency, high-finesse optical Fabry–Pérot cavity. The main difficulty with this approach has been the lack of strong coupling between the two disparate systems, something easily achieved with trapped ions. Recently, strong coupling was narrowly achieved with an optomechanical system[14] under large optical driving. Despite the strong coupling, this system was not in the quantum-enabled regime, as the thermal decoherence rate $\Gamma_{\rm th}$ was too large for observing quantum effects ($\Gamma_{\rm th} = n_{\rm m}\Gamma_{\rm m} \gg \kappa$, where κ and $\Gamma_{\rm m}$ are the intrinsic dissipation rates of the cavity and the mechanical oscillator, respectively). In this work, we describe a macroscopic, electromechanical system compatible with cryogenic operation that achieves a coupling rate g that is much greater than κ and $\Gamma_{\rm m}$. As this device operates in both quantum-enabled and strong-coupling regimes ($\Gamma_{\rm th} \ll \kappa < g < \Omega_{\rm m}$, where $\Omega_{\rm m}$ is the angular resonance frequency of the mechanical mode), it simultaneously fulfils all the requirements for observing and controlling many theoretically predicted quantum effects[2,3,7–9].

Cavity electromechanical systems operate under the same principles as their cavity optomechanical analogues. The motion of the mechanical oscillator modulates the frequency $\omega_{\rm c}$ of the optical or electromagnetic cavity. The single-photon coupling strength $g_0 = Gx_{\rm zp}$ is the product of $G = {\rm d}\omega_{\rm c}/{\rm d}x$ (the change in the cavity frequency for a given displacement x) and the zero point motion for mass m, given by $x_{\rm zp} = \sqrt{\hbar/2m\Omega_{\rm m}}$ ($\hbar$ is $h/2\pi$, where h is Planck's constant). In order to maximize the coupling, we would like to maximize the radiation pressure force per photon ($\hbar G$) and use a light mechanical object with a low resonant mode frequency $\Omega_{\rm m}$ (a soft spring constant). Optomechanical systems with silica microtoroids[11], dielectric membranes[15] and deflecting micromirrors[14] have all attempted to balance these preferred characteristics. The move to an electromechanical system has some advantages. These systems utilize low-loss superconducting circuits that are easily cooled to temperatures below 100 mK. Pioneering microwave electromechanical systems using parametric transducers achieved relatively large values of G and continue their development towards detection of gravitational waves[16,17]. Recent progress with lithographically fabricated microwave resonators[18] has focused on using nanowires to achieve large $x_{\rm zp}$, and has also enabled sideband cooling[19,20] and near quantum-limited detection[21,22], despite relatively weak coupling. Our approach, described below, takes advantage of the large capacitance produced by suspending an aluminium membrane approximately 50 nm above an aluminium base electrode (Fig. 1), to optimize both G and $x_{\rm zp}$ to achieve the largest g_0 to date.

Imagine two parallel metal plates of area A separated by a uniform vacuum gap d and electrically connected with a coiled wire (Fig. 1a, b). These plates form a capacitance $C = A\varepsilon_0/d$ (where ε_0 is the permittivity of free space) that electrically resonates with the inductance L of the coil at an angular frequency $\omega_{\rm c} = 1/\sqrt{LC}$. When the top plate is free to move a small distance $x \ll d$, then $G = {\rm d}\omega_{\rm c}/{\rm d}x \approx -\omega_{\rm c}/(2d)$. For a cavity with $\omega_{\rm c}/2\pi = 10$ GHz and a plate separation of 50 nm,

[1]National Institute of Standards and Technology, 325 Broadway, Boulder, Colorado 80305, USA.

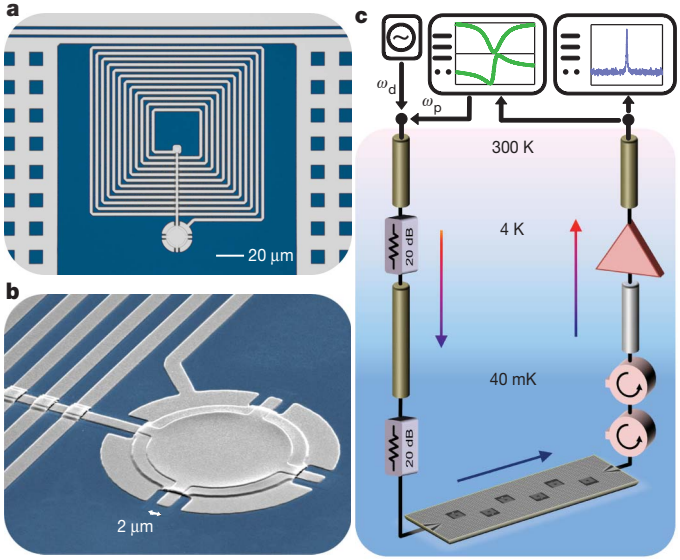

Figure 1 | Schematic description of the experiment. **a**, False-colour optical micrograph of the microwave resonator formed by a spiral inductor shunted by a parallel-plate capacitor. A coplanar waveguide transmission line (top) inductively couples microwave signals to and from the resonator (centre). **b**, False-colour scanning electron micrograph showing the upper plate of the capacitor suspended ~50 nm above the lower plate and free to vibrate like a taut, circular drum. The metallization is sputtered aluminium (grey) patterned on a sapphire substrate (blue). **c**, This circuit is measured by applying a microwave tone near the electrical resonance frequency through coaxial lines. Cryogenic attenuators (20 dB) on the input line and isolators (circular structures) on the output line ensure that thermal noise is reduced below the vacuum noise at microwave frequencies. The measured signal encoding the mechanical motion as modulation sidebands is transmitted to a low noise, cryogenic amplifier (triangle) via a superconducting coaxial cable and demodulated at room temperature with either a vector network analyser (green trace) or a spectrum analyser (blue trace).

$G/2\pi \approx 100\,\mathrm{MHz\,nm^{-1}}$. This is to be contrasted with previous experiments that used nanowires of very low mass and high aspect ratio[18–22]. These wires only contribute a fraction η (<1/1,000) of the total capacitance so that $G \approx -\eta\omega_c/(2d)$. So although these wires have large zero-point motion, the sensitivity is limited to $G/2\pi < 100\,\mathrm{kHz\,nm^{-1}}$.

Our circuit is fabricated with wafer-scale optical lithographic techniques developed for creating low-loss vacuum-gap-based microwave components[23]. The nearly circular membrane is 100 nm thick and has a diameter of 15 μm, allowing drum-like modes to resonate freely. The fundamental mode is $\Omega_m/2\pi = 10.69\,\mathrm{MHz}$, giving a zero-point motion of $x_{zp} = 4.1\,\mathrm{fm}$. The total capacitance $C \approx 38\,\mathrm{fF}$ combined with a parallel inductance, $L \approx 12\,\mathrm{nH}$, provides a fundamental microwave cavity resonance[23] of $\omega_c/2\pi \approx 7.5\,\mathrm{GHz}$. The device is cooled to 40 mK, far below the superconducting transition temperature of aluminium. To measure the motion of the membrane, we apply microwave signals through heavily attenuated coaxial lines, which inductively couple to the superconducting cavity, as shown schematically in Fig. 1c. The transmitted signals are amplified at 4 K with a cryogenic low-noise amplifier and demodulated at room temperature with either a commercial vector network analyser (for characterizing the cavity mode) or a spectrum analyser (for characterizing the mechanical mode).

Figure 2a shows the magnitude of transmission, $|T|^2$, near the cavity resonance at sufficiently low microwave power that radiation pressure effects can be neglected. A Lorentzian fit yields a resonance frequency of $\omega_c/2\pi = 7.47\,\mathrm{GHz}$ and a loaded intensity decay rate of $\kappa/2\pi = 170\,\mathrm{kHz}$. The depth of the dip at resonance shows that the circuit is overcoupled, so that the dominant source of damping is the intentional inductive coupling to the transmission line, $\kappa_{ex}/2\pi = 130\,\mathrm{kHz}$, which is much greater than the intrinsic decay rate, $\kappa_0/2\pi = 40\,\mathrm{kHz}$. The motion of the drum mode modulates the capacitance and thus the frequency of the electrical resonator, creating sidebands above and below the microwave drive frequency at $\omega_d \pm \Omega_m$. Figure 2b shows the noise power of the upper sideband due to the thermal motion of the drum at its fundamental mode, $\Omega_m/2\pi = 10.69\,\mathrm{MHz}$. These data show that the mechanical resonance has an intrinsic damping rate of $\Gamma_m/2\pi = 30\,\mathrm{Hz}$ and a high mechanical quality factor of $Q_m = 360{,}000$. Although the microscopic mechanisms responsible for mechanical dissipation need more investigation, these values are consistent with the improved Q-values associated with tensile stress found with aluminium nanowire-based oscillators[18,19,21]. With $\Omega_m/\kappa = 63$, it is clear that we are deeply within the resolved-sideband regime where the mechanical resonance frequency is much larger than the cavity linewidth: this is a prerequisite for both sideband cooling to the ground state and for observing normal-mode splitting[7–9].

The quantum-mechanical behaviour of this parametrically coupled system is described by the interaction Hamiltonian, $H_I = -\hbar a^\dagger a g_0(b^\dagger + b)$, where $a^\dagger$ (a) and $b^\dagger$ (b) are the creation (annihilation) operators for photons and phonons, respectively. Because the motion of this drum strongly influences ω_c, microwave signals can be used not only to detect the motion of the oscillator but also to impart back-action forces on it. The radiation pressure force of the microwave drive photons gives rise to 'optical' spring and damping effects. The interaction Hamiltonian can be linearized in a frame co-rotating with the drive, taking the form, $H_I = -\hbar g(a^\dagger + a)(b^\dagger + b)$, where $g = g_0\sqrt{n_d}$ is the total (linearized optomechanical) coupling strength[7–9], and n_d is

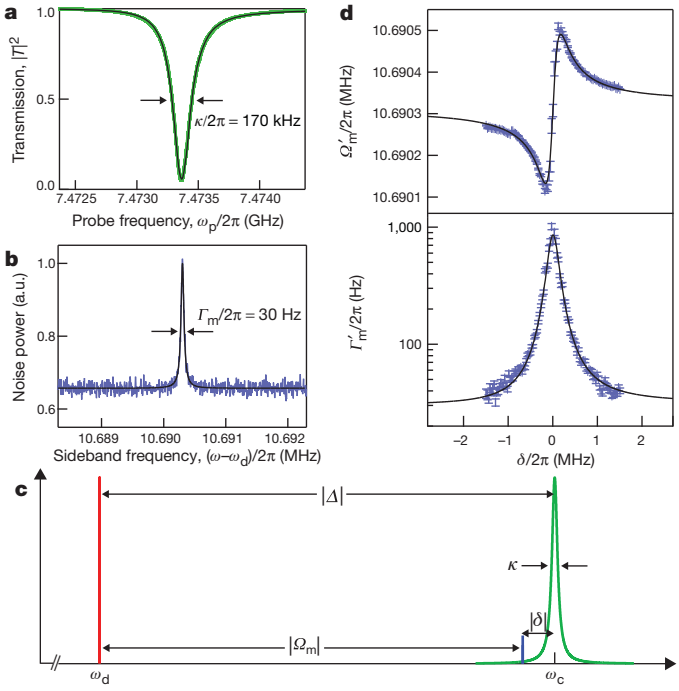

Figure 2 | Characterization of mechanical and microwave resonances. **a**, Measured probe transmission spectrum (green) and Lorentzian fit (black) of the microwave circuit at low power, where optomechanical effects are negligible. The width of the resonance yields the overcoupled, intensity decay rate $\kappa/2\pi = 170\,\mathrm{kHz}$. **b**, The mechanical resonance manifests itself as a peak in the noise spectrum (blue), which appears Ω_m above and below the microwave drive frequency, owing to the thermal motion of the drum up- or down-converting microwave photons. At low microwave power, where back-action effects are negligible, the Lorentzian fit (black) yields an intrinsic mechanical dissipation rate $\Gamma_m/2\pi = 30\,\mathrm{Hz}$ ($Q_m = 360{,}000$). **c**, Schematic diagram for the relative frequencies of the microwave drive (red) and the upper mechanical sideband (blue) with respect to the narrow cavity resonance (green). **d**, The modified mechanical resonance frequency Ω'_m and damping rate Γ'_m as a function of the relative detuning δ fit well to the theory of dynamical back-action (black), yielding $G/2\pi = 56 \pm 7\,\mathrm{MHz\,nm^{-1}}$.

the number of drive photons in the cavity. If the drive is detuned so that its upper mechanical sideband is near the cavity resonance, $\delta = (\omega_d + \Omega_m) - \omega_c \ll \Omega_m$ (Fig. 2c), the modified mechanical resonance frequency Ω'_m and damping rate Γ'_m closely follow the imaginary and real parts of the cavity response. In the resolved sideband regime these quantities are well approximated by[7,8,24]:

$$\Omega'_m \approx \Omega_m + \frac{4g^2\delta}{\kappa^2 + 4\delta^2} \quad (1)$$

$$\Gamma'_m \approx \Gamma_m + \frac{4g^2\kappa}{\kappa^2 + 4\delta^2} \quad (2)$$

Figure 2d shows the measured effects of this dynamical back-action on the drum as a function of δ. The incident microwave power P_{in} is held constant at 10 pW. As this power is applied very far from the cavity resonance, it results in a greatly reduced number of photons in the cavity, given by $n_d = (2P_{in}\kappa_{ex}/\hbar\omega_d)/(\kappa^2 + 4\Delta^2)$, where $\Delta = \omega_d - \omega_c$. Even for this moderate-power microwave drive with $n_d \leq 800$, the effects on the mechanical oscillator are quite striking; the intrinsic mechanical damping is dominated by the damping from the microwave photons. Knowing n_d and estimating x_{zp} from geometry, we can fit these data to equations (1) and (2) (shown in black in Fig. 2d) to extract $G/2\pi = 56 \pm 7$ MHz nm^{-1}.

Just as the microwave photons strongly affect the mechanical mode, the symmetry of the parametric interaction suggests that the mechanics should influence the cavity mode. To investigate this, we apply both a microwave drive tone ω_d and a second probe tone ω_p. Here, the drive tone will induce an interaction between the mechanics and the cavity, while the probe tone will monitor the response of the cavity. This technique provides a way to measure the spectroscopy of the 'dressed' cavity states in the presence of the electromechanical interaction. Figure 3a shows a series of cavity probe spectra taken with successively higher microwave power applied with $\Delta = -\Omega_m$. Once the drive power is large enough that $g \approx \sqrt{\Gamma_m \kappa}$, the mechanical sideband of the driving field appears in the cavity response function. As n_d, and hence g, increase, so does the normalized probe transmission at the cavity resonance, $|T(\omega_c)|$. The width of this peak also increases and is given by the modified mechanical damping rate in equation (2). This electromechanical effect can be understood as the result of a radiation pressure force at the beat frequency between the drive and probe photons, which drives the motion of the drum near its resonance frequency. The driven motion results in a mechanical sideband on the drive field that can interfere with the probe field and hence modifies the probe spectrum. This interference is the mechanical analogue of electromagnetically induced transparency[25], which is well known in atomic physics and has enabled such innovations as slow light and photon storage. Recently, these effects have been addressed in the context of optomechanics, both theoretically[10,11] and experimentally[11]. The analogous effect is demonstrated here for the first time in an electromechanical system. For our electrical circuit, the transmission spectrum is[10,11]:

$$T = 1 - \frac{\kappa_{ex}(1 - j\chi)}{\kappa + 2j(\omega_p - \omega_c) + 4\chi(\omega_d - \omega_c)} \quad (3)$$

where

$$\chi = \frac{4g^2\Omega_m}{\left[\kappa + 2j(\omega_p - 2\omega_d + \omega_c)\right]\left[\Omega_m^2 - (\omega_p - \omega_d)^2 + j(\omega_p - \omega_d)\Gamma_m\right]}$$

At high enough power, Γ'_m becomes comparable to or greater than κ, at which point equations (1) and (2) are no longer valid. This is precisely the point at which the driven system enters the strong-coupling regime, in which the coupling exceeds the intrinsic dissipation in either of the original modes ($g \geq \kappa \gg \Gamma_m$). The eigenmodes of the driven, coupled system are now hybrids of the original radio-frequency mechanical resonance and the microwave electrical resonance. The

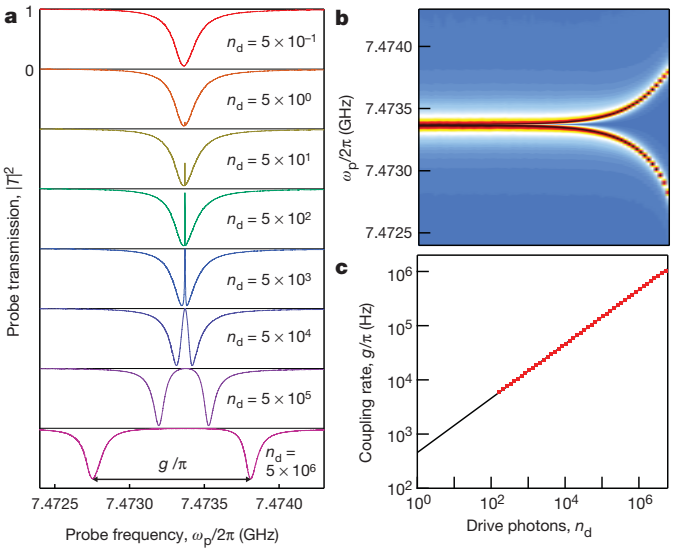

Figure 3 | Demonstration of the strong-coupling regime. **a**, Normalized microwave cavity transmission in the presence of a microwave drive applied with $\Delta = -\Omega_m$, with successive plots for increasing drive amplitude n_d. At moderate drive amplitude ($n_d \approx 10$), the interference between the drive and probe photons results in a narrow peak in the cavity spectrum, whose width is given by the mechanical linewidth Γ'_m. This represents the onset of electromechanically induced transparency[11]. When Γ'_m becomes comparable to κ, the cavity resonance splits into normal modes. The eigenmodes of the system are no longer purely electrical or mechanical, but are a pair of hybrid electromechanical resonances. **b**, The transmission as a function of probe frequency and number of drive photons shows that the driven system enters the strong-coupling regime ($g \geq \kappa, \Gamma_m$). Here, the logarithmic colour scale show the transmission as it varies from −13 dB (dark red) to 0 dB (blue). **c**, The measured coupling rate g (red) follows the expected dependence on the number of drive photons, with a fit to $\sqrt{n_d}$ shown in black.

system exhibits the well-known normal-mode splitting of two strongly coupled harmonic oscillators. This effect is observed through the cavity response instead of the mechanical response as is done in other experiments[14]. For our device, progression into the strong-coupling regime is shown in Fig. 3a, b with a crossover occurring at $n_d \approx 10^5$. In this regime, the damping rate of each of the two normal modes approaches $(\kappa + \Gamma_m)/2$, and the coupling results in a splitting of $2g$. In Fig. 3c, g is extracted by fitting each spectrum at a given drive power to equation (3). The splitting shows $\sqrt{n_d}$ dependence, with a single-photon coupling rate of $g_0/\pi = 460$ Hz. At the highest drive power, $n_d = 5 \times 10^6$, the splitting is $g/\pi = 1$ MHz, exceeding both κ and Γ_m. The cooperativity $C = 4g^2/\Gamma_m\kappa$ represents a good figure of merit for an opto- or electromechanical system, regardless of its detailed construction. For our system, we find a maximum cooperativity of $C \approx 200{,}000$, beyond those previously achieved[11,14,15,20,21].

By measuring the in-phase and quadrature components of the transmitted probe signal, we determine the real and imaginary parts of the cavity spectrum in the presence of the electromechanical interactions. We find excellent agreement between theory and experiment for both magnitude and phase over the entire range of accessible detunings and powers. Figure 4a shows the magnitude and phase of the probe transmission for three arbitrary values of δ when $g/\pi = 150$ kHz. The black lines are fits to the magnitude and argument of equation (3). The narrow resonance resulting from the mechanical interaction could be used as a tunable delay for microwave signals[11], with a maximum group delay of ~5 ms. Two-dimensional plots of $|T|$ are shown in Fig. 4 as a function of both ω_d and ω_p. At low drive amplitude (Fig. 4b), the narrow mechanical sideband appears as a sharp dip or peak in transmission whenever $\omega_p = \omega_d + \Omega'_m$. As the drive amplitude is increased (Fig. 4c), the dispersive coupling between the normal modes becomes apparent. Although the mechanical sideband is narrow when it is far

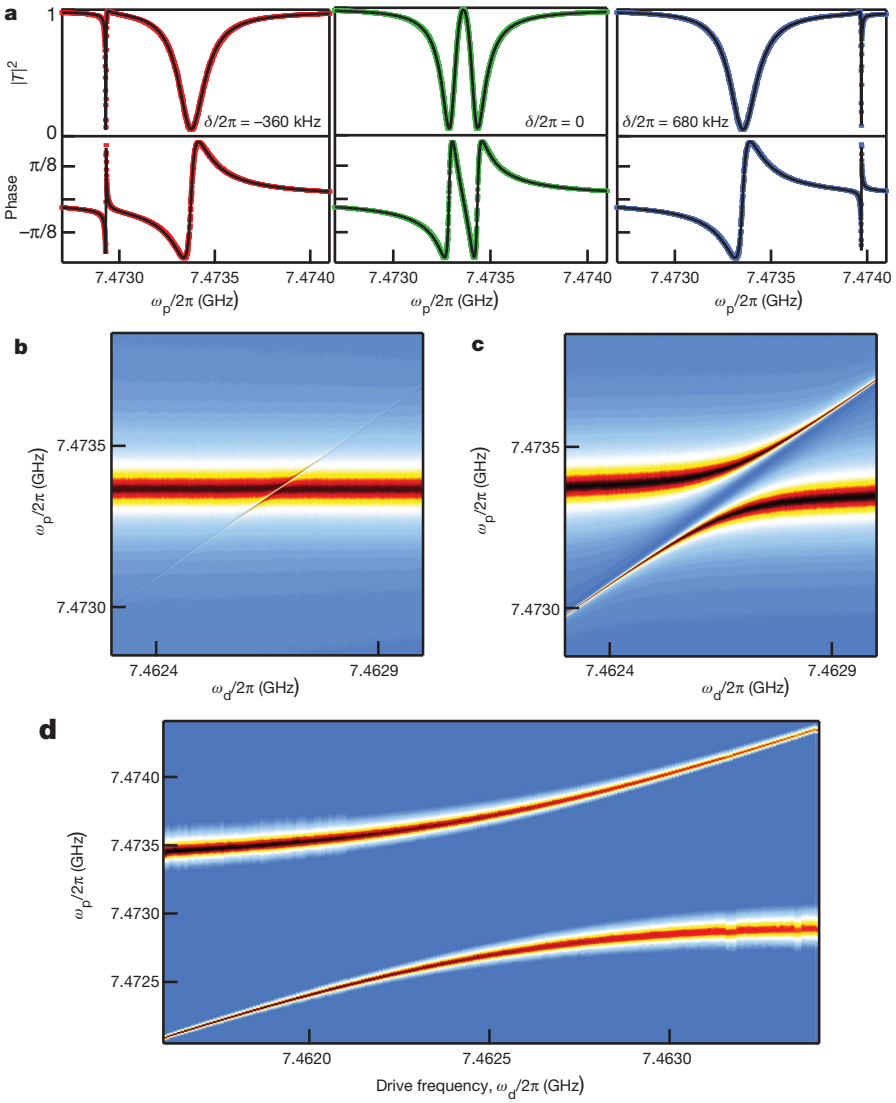

Figure 4 | Spectroscopy in the strong-coupled regime. **a**, The normalized magnitude and phase of the cavity transmission in the presence of a strong microwave drive. The data shown in red, green and blue are for three different detunings δ with fits to equation (3) (black). **b**, For relatively low drive power ($n_d \approx 10$), the mechanical sideband appears as a sharp dip or peak in the probe transmission at a frequency $\omega_d + \Omega'_m$. **c**, When the drive amplitude is increased ($n_d \approx 10^4$), the two resonances show an avoided crossing between the eigenmodes of the coupled system. **d**, For the largest amplitude drive ($n_d \approx 5 \times 10^6$), the driven transmission spectra are split by much more than κ or Γ_m for a broad range of detunings.

from resonance, it inherits the cavity's larger damping rate as it approaches ω_c. At the largest coupling, the normal-mode splitting is appreciable for a broad range of drive and probe frequencies (Fig. 4d).

This experiment demonstrates that by engineering a microwave resonant circuit with a free-standing micromechanical membrane or drum, a large coupling is possible without degradation of either the mechanical or electromagnetic quality factors. Our measurements have shown clear quantitative agreement with theoretical predictions for dynamical back-action and normal-mode splitting, with the latter being exceptionally large, namely 10% of Ω_m. Simple refinements—such as reducing d, using thinner membranes or exploring higher-order modes—could further enhance the coupling strength and relax cooling requirements. This new system shows the performance necessary to not only observe quantum effects but also (with additional circuitry) enable the realization of a number of important goals. For continuous measurements, these include detection of zero-point motion[1], evading quantum back-action[22] or Heisenberg-limited detection of displacement or force[1], preparation of non-classical photon states through motional effects[3], and possibly a direct quantum non-demolition x^2 energy measurement[15]. Discrete measurements would enable the preparation of complex multi-phonon states[26], long-lived quantum memory, a quantum bus architecture for quantum information processing analogous to that achieved with ion traps, and a way to investigate decoherence for large, spatially separated superposition states[27].

Last, we consider ground-state cooling, which is the next step forward. Assuming thermal equilibrium at a base cryostat temperature of 20 mK, we expect the cavity to be in its ground state and the thermal occupancy of the mechanical mode to be $n_m \approx 40$ quanta. Strong coupling implies that resolved sideband cooling can be used to reduce the occupancy of the mechanical mode by a factor of $\kappa/\Gamma_m \approx 5{,}000$ (refs 7–9), placing both (coupled) resonators in their ground state. Once this is achieved, the thermal lifetime of a single phonon would be $1/\Gamma_{th} \approx 130\,\mu s$, which is orders of magnitude longer than typical superconducting qubit lifetimes. Verifying this achievement would require either a better cryogenic amplifier[21,28] (for continuous measurements) or a superconducting qubit[4] (for discrete measurements). Continuous measurement with microwave parametric amplifiers, which achieve nearly quantum-limited sensitivity, reduce by a factor of 1,000 the integration time necessary to resolve mechanical occupancy below the single phonon level[21]. Alternatively, if a qubit were strongly coupled to the microwave cavity[4,26], a single photon could be

exchanged with the qubit over a time of $\sim$10 ns and would survive there for nearly $1/\kappa_0 \approx 4\,\mu s$. For the largest coupling strengths achieved here, the microwave photon could then be converted into a phonon (and vice versa) in approximately $\pi/2g \approx 0.5\,\mu s$, which is adequate for building up multi-phonon states[26,29]. Beyond this, proposals exist that would allow the mechanical drum to convert microwave photon states to optical photon states, which can be used to transmit quantum information at room temperature[30].

Received 31 October 2010; accepted 31 January 2011.

1. Braginsky, V. B. & Khalili, F. Y. *Quantum Measurement* (Cambridge Univ. Press, 1992).
2. Mancini, S., Man'ko, V. I. & Tombesi, P. Ponderomotive control of quantum macroscopic coherence. *Phys. Rev. A* **55,** 3042–3050 (1997).
3. Bose, S., Jacobs, K. & Knight, P. L. Preparation of nonclassical states in cavities with a moving mirror. *Phys. Rev. A* **56,** 4175–4186 (1997).
4. O'Connell, A. D. *et al.* Quantum ground state and single-phonon control of a mechanical resonator. *Nature* **464,** 697–703 (2010).
5. Kippenberg, T. J. & Vahala, K. J. Cavity optomechanics: back-action at the mesoscale. *Science* **321,** 1172–1176 (2008).
6. Marquardt, F. & Girvin, S. M. Optomechanics. *Physics* **2,** 40 (2009).
7. Marquardt, F., Chen, J. P., Clerk, A. A. & Girvin, S. M. Quantum theory of cavity-assisted sideband cooling of mechanical motion. *Phys. Rev. Lett.* **99,** 093902 (2007).
8. Wilson-Rae, I., Nooshi, N., Zwerger, W. & Kippenberg, T. J. Theory of ground state cooling of a mechanical oscillator using dynamical backaction. *Phys. Rev. Lett.* **99,** 093901 (2007).
9. Dobrindt, J. M., Wilson-Rae, I. & Kippenberg, T. J. Parametric normal-mode splitting in cavity optomechanics. *Phys. Rev. Lett.* **101,** 263602 (2008).
10. Agarwal, G. S. & Huang, S. Electromagnetically induced transparency in mechanical effects of light. *Phys. Rev. A* **81,** 041803 (2010).
11. Weis, S. *et al.* Optomechanically induced transparency. *Science* **330,** 1520–1523 (2010).
12. Ekinci, K. L. & Roukes, M. L. Nanoelectromechanical systems. *Rev. Sci. Instrum.* **76,** 061101 (2005).
13. Diedrich, F., Bergquist, J. C., Itano, W. M. & Wineland, D. J. Laser cooling to the zero-point energy of motion. *Phys. Rev. Lett.* **62,** 403–406 (1989).
14. Gröblacher, S., Hammerer, K., Vanner, M. R. & Aspelmeyer, M. Observation of strong coupling between a micromechanical resonator and an optical cavity field. *Nature* **460,** 724–727 (2009).
15. Thompson, J. D. *et al.* Strong dispersive coupling of a high-finesse cavity to a micromechanical membrane. *Nature* **452,** 72–75 (2008).
16. Braginsky, V. B., Manukin, A. B. & Tikhonov, M. Y. Investigation of dissipative ponderomotive effects of electromagnetic radiation. *Sov. Phys. JETP* **31,** 829–830 (1970).
17. Linthorne, N. P., Veitch, P. J. & Blair, D. G. Interaction of a parametric transducer with a resonant bar gravitational radiation detector. *J. Phys. D* **23,** 1–6 (1990).
18. Regal, C. A., Teufel, J. D. & Lehnert, K. W. Measuring nanomechanical motion with a microwave cavity interferometer. *Nature Phys.* **4,** 555–560 (2008).
19. Teufel, J. D., Harlow, J. W., Regal, C. A. & Lehnert, K. W. Dynamical backaction of microwave fields on a nanomechanical oscillator. *Phys. Rev. Lett.* **101,** 197203 (2008).
20. Rocheleau, T. *et al.* Preparation and detection of a mechanical resonator near the ground state of motion. *Nature* **463,** 72–75 (2010).
21. Teufel, J. D., Donner, T., Castellanos-Beltran, M. A., Harlow, J. W. & Lehnert, K. W. Nanomechanical motion measured with an imprecision below that at the standard quantum limit. *Nature Nanotechnol.* **4,** 820–823 (2009).
22. Hertzberg, J. B. *et al.* Back-action-evading measurements of nanomechanical motion. *Nature Phys.* **6,** 213–217 (2010).
23. Cicak, K. *et al.* Low-loss superconducting resonant circuits using vacuum-gap-based microwave components. *Appl. Phys. Lett.* **96,** 093502 (2010).
24. Blencowe, M. P. & Buks, E. Quantum analysis of a linear dc squid mechanical displacement detector. *Phys. Rev. B* **76,** 014511 (2007).
25. Boller, K.-J., Imamolu, A. & Harris, S. E. Observation of electromagnetically induced transparency. *Phys. Rev. Lett.* **66,** 2593–2596 (1991).
26. Hofheinz, M. *et al.* Synthesizing arbitrary quantum states in a superconducting resonator. *Nature* **459,** 546–549 (2009).
27. Marshall, W., Simon, C., Penrose, R. & Bouwmeester, D. Towards quantum superpositions of a mirror. *Phys. Rev. Lett.* **91,** 130401 (2003).
28. Castellanos-Beltran, M. A., Irwin, K. D., Hilton, G. C., Vale, L. R. & Lehnert, K. W. Amplification and squeezing of quantum noise with a tunable Josephson metamaterial. *Nature Phys.* **4,** 929–931 (2008).
29. Akram, U., Kiesel, N., Aspelmeyer, M. & Milburn, G. J. Single-photon opto-mechanics in the strong coupling regime. *N. J. Phys.* **12,** 083030 (2010).
30. Regal, C. A. & Lehnert, K. W. From cavity electromechanics to cavity optomechanics. *J. Phys. Conf. Ser.* **264,** 012025 (2011).

Acknowledgements We thank A. W. Sanders for taking the micrograph in Fig. 1b, and acknowledge discussions with T. Donner, J. H. Harlow and K. W. Lehnert. This paper is a contribution by the National Institute of Standards and Technology and not subject to US copyright.

Author Contributions J.D.T. and R.W.S. conceived the device. J.D.T. designed the circuit. J.D.T. and D.L. fabricated the devices. J.D.T. performed and analysed the measurements. R.W.S. oversaw all aspects of this work. All authors provided experimental support and commented on the manuscript.

Author Information Reprints and permissions information is available at www.nature.com/reprints. The authors declare no competing financial interests. Readers are welcome to comment on the online version of this article at www.nature.com/nature. Correspondence and requests for materials should be addressed to J.D.T. (john.teufel@nist.gov).